



Quantum tomography via the *MaxEnt* principle

VLADIMÍR BUŽEK†‡ and GABRIEL DROBNÝ†

† Institute of Physics, Slovak Academy of Sciences, Dúbravská cesta 9, 842 28 Bratislava, Slovakia

‡ Faculty of Informatics, Masaryk University, Botanická 68a, Brno 602 00, Czech Republic

(Received 17 April 2000)

Abstract. We show how the maximum entropy (*MaxEnt*) principle can be efficiently used for a reconstruction of quantum states of light from incomplete tomographic data. This *MaxEnt* reconstruction scheme is several orders more efficient than the standard inverse Radon transformation or the reconstruction via direct sampling using pattern functions.

1. Introduction

Quantum-state reconstruction schemes can be understood as an *a posteriori* estimation of the density operator of a given quantum-mechanical (microscopic) system based on data obtained with the help of a macroscopic measurement apparatus [1]. The quality of the reconstruction depends on the 'quality' of the measured data and the efficiency of the reconstruction procedure with the help of which the data analysis is performed.

Providing all system observables (the complete observation level or the quorum of observables [2, 3]) have been precisely measured, then the density operator of a quantum-mechanical system can be precisely reconstructed. A typical example of such deterministic reconstruction is quantum homodyne tomography (see section 2).

On the other hand, if just a subset \hat{G}_ν ($\nu = 1, 2, \dots, n$) of observables from the quorum (this subset constitutes the so-called observation level [4]) is measured then the complete information about the system is not available. Therefore one needs an additional criterion which would help to reconstruct (estimate) the density operator uniquely in a most reliable way.

The Jaynes principle of the maximum entropy (the so-called *MaxEnt* principle) [4] (see also [5–7]) serves as the desired criterion. We will show in the paper that the *MaxEnt* principle provides us with a very efficient prescription how to reconstruct density operators of quantum-mechanical systems from mean values of a given set of observables. We will show that when applied to incomplete tomographic data the reconstruction of density operators via the *MaxEnt* principle is several orders more efficient than the standard reconstruction via the inverse Radon transformation or the direct sampling via the pattern functions.

This paper is organized as follows. In section 2 we briefly describe the tomographic reconstruction of Wigner functions of a single-mode light field. In section 3 we introduce the Jaynes principle of Maximum Entropy and we show its

connection to quantum tomography. Numerical reconstruction of Wigner functions from incomplete tomographic data is analysed in section 4. We summarize our results in section 5.

2. Tomographic reconstruction of quantum states of light

Utilizing a close analogy between the operator for the electric component $\hat{E}(r, t)$ of a monochromatic light field and the quantum-mechanical harmonic oscillator we will consider a dynamical system which is described by a pair of canonically conjugated Hermitean observables \hat{q} and \hat{p} ,

$$[\hat{q}, \hat{p}] = i\hbar. \quad (1)$$

Eigenvalues of these operators range continuously from $-\infty$ to $+\infty$. The annihilation and creation operators \hat{a} and \hat{a}^\dagger can be expressed as a complex linear combination of \hat{q} and \hat{p} :

$$\hat{a} = \frac{1}{(2\hbar)^{1/2}} (\lambda\hat{q} + i\lambda^{-1}\hat{p}); \quad \hat{a}^\dagger = \frac{1}{(2\hbar)^{1/2}} (\lambda\hat{q} - i\lambda^{-1}\hat{p}), \quad (2)$$

where λ is a real parameter. The operators \hat{a} and \hat{a}^\dagger obey the Weyl–Heisenberg commutation relation

$$[\hat{a}, \hat{a}^\dagger] = 1, \quad (3)$$

and therefore possess the same algebraic properties as the operator associated with the complex amplitude of a harmonic oscillator (in this case $\lambda = (m\omega)^{1/2}$, where m and ω are the mass and the frequency of the quantum-mechanical oscillator, respectively) or the photon annihilation and creation operators of a single mode of the quantum electromagnetic field. In this case $\lambda = (\epsilon_0\omega)^{1/2}$ (ϵ_0 is the dielectric constant and ω is the frequency of the field mode) and the operator for the electric field reads (we do not take into account polarization of the field)

$$\hat{E}(r, t) = 2^{1/2}\mathcal{E}_0(\hat{a} \exp(-i\omega t) + \hat{a}^\dagger \exp(i\omega t))u(r), \quad (4)$$

where $u(r)$ describes the spatial field distribution and is the same in both classical and quantum theories. The constant $\mathcal{E}_0 = (\hbar\omega/2\epsilon_0V)^{1/2}$ is equal to the ‘electric field per photon’ in the cavity of volume V .

The Wigner function [8] can be defined as a particular Fourier transform of the density operator $\hat{\rho}$ of a harmonic oscillator expressed in the basis of the eigenvectors $|q\rangle$ of the position operator \hat{q} :

$$W_{\hat{\rho}}(q, p) \equiv \int_{-\infty}^{\infty} d\zeta \langle q - \zeta/2 | \hat{\rho} | q + \zeta/2 \rangle \exp(ip\zeta/\hbar). \quad (5)$$

Alternatively, the Wigner function (WF) can be rewritten in the form

$$W_{\hat{\rho}}(q, p) = \frac{1}{2\pi\hbar} \int C_{\hat{\rho}}^{(W)}(q', p') \exp\left[-\frac{i}{\hbar}(qp' - pq')\right] dq' dp', \quad (6)$$

where the characteristic function $C_{\hat{\rho}}^{(W)}(q, p)$ is given by the relation

$$C_{\hat{\rho}}^{(W)}(q, p) = \text{Tr}[\hat{\rho}\hat{D}(q, p)]. \quad (7)$$

The displacement operator $\hat{D}(q, p)$ in terms of the position and the momentum operators reads

$$\hat{D}(q, p) = \exp \left[\frac{i}{\hbar} (\hat{q}p - \hat{p}q) \right]. \tag{8}$$

The Wigner function can be interpreted as the quasiprobability density distribution through which a probability can be expressed to find a quantum-mechanical system (harmonic oscillator) around the 'point' (q, p) of the phase space. With the help of the Wigner function $W_{\hat{\rho}}(q, p)$ the position and momentum probability distributions $w_{\hat{\rho}}(q)$ and $w_{\hat{\rho}}(p)$ can be expressed from $W_{\hat{\rho}}(q, p)$ via marginal integration over the conjugated variable (in what follows we assume $\lambda = 1$)

$$w_{\hat{\rho}}(q) \equiv \frac{1}{(2\pi\hbar)^{1/2}} \int dp W_{\hat{\rho}}(q, p) = (2\pi\hbar)^{1/2} \langle q | \hat{\rho} | q \rangle, \tag{9}$$

where $|q\rangle$ is the eigenstate of the position operator \hat{q} . The marginal probability distribution $w_{\hat{\rho}}(q)$ is normalized to unity, i.e.

$$\frac{1}{(2\pi\hbar)^{1/2}} \int dq w_{\hat{\rho}}(q) = 1. \tag{10}$$

As an illustration let us consider a Wigner function of a specific superposition of two coherent states:

$$|\alpha_e\rangle = N_e^{1/2} (|\alpha\rangle + |-\alpha\rangle); \quad N_e^{-1} = 2[1 + \exp(-2|\alpha|^2)], \tag{11}$$

which is called the even coherent state [9]. The coherent state $|\alpha\rangle$ is defined as, usually, $|\alpha\rangle = \hat{D}(\bar{q}, \bar{p})|0\rangle$, where $|0\rangle$ is the vacuum state of the harmonic oscillator. The parameter $\alpha = \alpha_x + i\alpha_y$, is defined via the relations $\bar{q} = (2\hbar)^{1/2}\alpha_x/\lambda$ and $\bar{p} = (2\hbar)^{1/2}\alpha_y\lambda$. The Wigner function of the coherent state $|\alpha\rangle$ has a Gaussian form

$$W_{|\alpha\rangle}(q, p) = \frac{1}{\sigma_q \sigma_p} \exp \left[-\frac{1}{2\hbar} \frac{(q - \bar{q})^2}{\sigma_q^2} - \frac{1}{2\hbar} \frac{(p - \bar{p})^2}{\sigma_p^2} \right], \tag{12}$$

where

$$\sigma_q^2 = \frac{1}{2\lambda^2} \quad \text{and} \quad \sigma_p^2 = \frac{\lambda^2}{2}. \tag{13}$$

If we assume α to be real, then the Wigner function of the even coherent state reads

$$W_{|\alpha_e\rangle}(q, p) = N_e [W_{|\alpha\rangle}(q, p) + W_{|-\alpha\rangle}(q, p) + W_{\text{int}}(q, p)]; \tag{14}$$

where $W_{|\pm\alpha\rangle}(q, p)$ is the WF of coherent states $|\pm\alpha\rangle$. The interference part of the Wigner function (14) is given by the relation

$$W_{\text{int}}(q, p) = \frac{2}{\sigma_q \sigma_p} \exp \left[-\frac{q^2}{2\hbar\sigma_q^2} - \frac{p^2}{2\hbar\sigma_p^2} \right] \cos \left(\frac{\bar{q}p}{\hbar\sigma_q\sigma_p} \right), \tag{15}$$

We plot the Wigner function of the even coherent state in figure 1 (a). From the figure it is clearly seen that the interference term (15) results in oscillations of the Wigner function around the origin of the phase space.

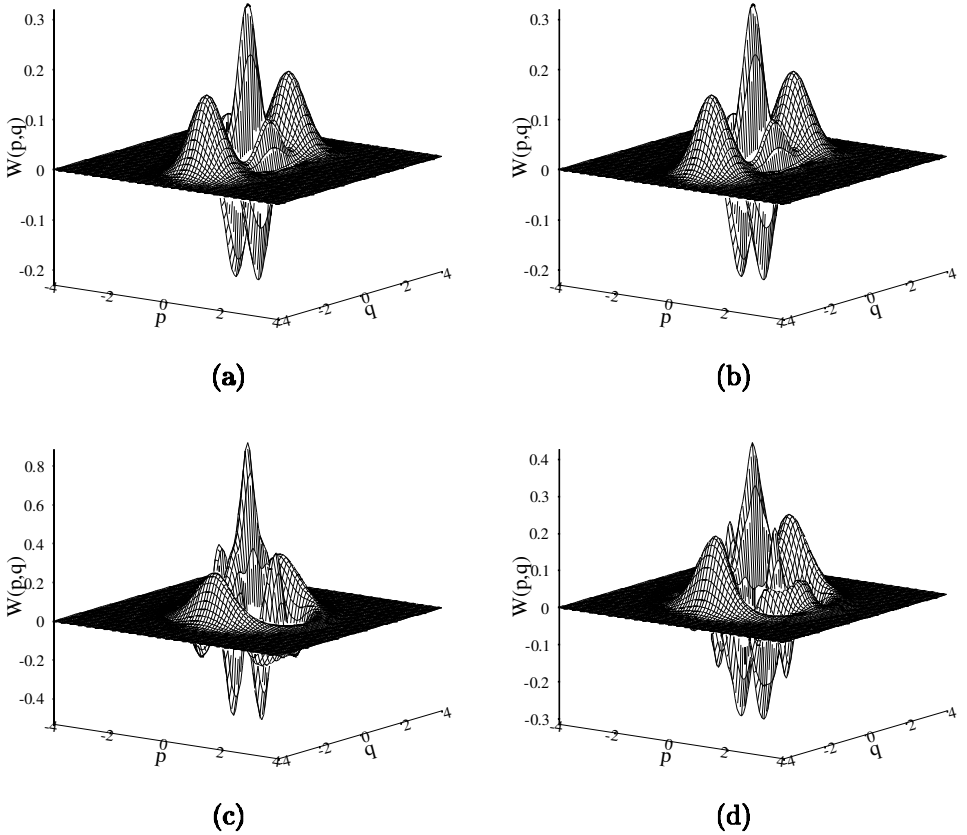


Figure 1. (a) The Wigner function of the even coherent state with $\alpha = 2$. (b) Reconstruction of the Wigner function via the *MaxEnt* principle from two marginal distributions ($N_\theta = 2$) for the position and momentum. The measured marginal distributions are divided into $N_x = 40$ bins of width $\Delta x = 0.2$ covering the interval $\langle -4, 4 \rangle$. The fidelity of the reconstruction is $\Delta Q = 5.4 \times 10^{-12}$ and $\Delta \rho = 1.0 \times 10^{-8}$, the corresponding entropy is $S \approx 10^{-6}$. (c) Optical tomography via direct sampling using pattern functions with $N_\theta = 2$ and with an artificial truncation at $N_{\max} = 4$. This value of N_{\max} is chosen such that the deviation ΔQ is minimized. In this case $\Delta Q \approx 9.17$ and $\Delta \rho \approx 3.7$. The reconstructed Wigner function is unphysical because the corresponding density operator has negative probabilities for odd Fock states ($P_1 \approx -0.35$, $P_3 \approx -0.54$). (d) The result of the tomography can be improved when the number of quadratures is larger. For $N_\theta = 4$ and the truncation at $N_{\max} = 6$ we can improve the fidelity of the reconstruction ($\Delta Q \approx 1.33$ and $\Delta \rho = 0.51$) but it is still unphysical because $P_1 \approx -0.1$.

2.1. Quantum homodyne tomography

Relation (9) for the probability distribution $w_\rho(q)$ of the position operator \hat{q} can be generalized to the case of the distribution of the rotated quadrature operator \hat{x}_θ . This operator is defined as

$$\hat{x}_\theta = \left(\frac{\hbar}{2}\right)^{1/2} [\hat{a} \exp(-i\theta) + \hat{a}^\dagger \exp(i\theta)], \quad (16)$$

and the corresponding conjugated operator $\hat{x}_{\theta+\pi/2}$, such that $[\hat{x}_\theta, \hat{x}_{\theta+\pi/2}] = i\hbar$, reads

$$\hat{x}_{\theta+\pi/2} = \frac{\hbar^{1/2}}{i2^{1/2}}[\hat{a} \exp(-i\theta) - \hat{a}^\dagger \exp(i\theta)]. \tag{17}$$

The position and the momentum operators are related to the operator \hat{x}_θ as, $\hat{q} = \hat{x}_0$ and $\hat{x}_{\pi/2} = \hat{p}$. The rotation (i.e. the linear homogeneous canonical transformation) given by equations (16) and (17) can be performed by the unitary operator $\hat{U}(\theta)$:

$$\hat{U}(\theta) = \exp[-i\theta\hat{a}^\dagger\hat{a}], \tag{18}$$

so that

$$\hat{x}_\theta = \hat{U}^\dagger(\theta)\hat{x}_0\hat{U}(\theta); \quad \hat{x}_{\theta+\pi/2} = \hat{U}^\dagger(\theta)\hat{x}_{\pi/2}\hat{U}(\theta). \tag{19}$$

Alternatively, in the vector formalism we can rewrite the transformation (19) as

$$\begin{pmatrix} \hat{x}_\theta \\ \hat{x}_{\theta+\pi/2} \end{pmatrix} = \mathbf{F} \begin{pmatrix} \hat{q} \\ \hat{p} \end{pmatrix}; \quad \mathbf{F} = \begin{pmatrix} \cos \theta & \sin \theta \\ -\sin \theta & \cos \theta \end{pmatrix}. \tag{20}$$

Eigenvalues x_θ and $x_{\theta+\pi/2}$ of the operators \hat{x}_θ and $\hat{x}_{\theta+\pi/2}$ can be expressed in terms of the eigenvalues q and p of the position and momentum operators as:

$$\begin{pmatrix} x_\theta \\ x_{\theta+\pi/2} \end{pmatrix} = \mathbf{F} \begin{pmatrix} q \\ p \end{pmatrix}; \quad \begin{pmatrix} q \\ p \end{pmatrix} = \mathbf{F}^{-1} \begin{pmatrix} x_\theta \\ x_{\theta+\pi/2} \end{pmatrix};$$

$$\mathbf{F}^{-1} = \begin{pmatrix} \cos \theta & -\sin \theta \\ \sin \theta & \cos \theta \end{pmatrix}, \tag{21}$$

where the matrix \mathbf{F} is given by equation (20) and \mathbf{F}^{-1} is the corresponding inverse matrix. It has been shown by Ekert and Knight [10] that Wigner functions are transformed under the action of the linear canonical transformation (20) as:

$$\begin{aligned} W_{\hat{\rho}}(q,p) &\rightarrow W_{\hat{\rho}}(\mathbf{F}^{-1}(x_\theta, x_{\theta+\pi/2})) \\ &= W_{\hat{\rho}}(x_\theta \cos \theta - x_{\theta+\pi/2} \sin \theta; x_\theta \sin \theta + x_{\theta+\pi/2} \cos \theta), \end{aligned} \tag{22}$$

which means that the probability distribution $w_{\hat{\rho}}(x_\theta, \theta) = (2\pi\hbar)^{1/2} \langle x_\theta | \hat{\rho} | x_\theta \rangle$ can be evaluated as

$$\begin{aligned} w_{\hat{\rho}}(x_\theta, \theta) &= \frac{1}{(2\pi\hbar)^{1/2}} \int_{-\infty}^{\infty} dx_{\theta+\pi/2} \\ &\times W_{\hat{\rho}}(x_\theta \cos \theta - x_{\theta+\pi/2} \sin \theta; x_\theta \sin \theta + x_{\theta+\pi/2} \cos \theta). \end{aligned} \tag{23}$$

As shown by Vogel and Risken [11] (see also [12–15]) the knowledge of $w_{\hat{\rho}}(x_\theta, \theta)$ for all values of θ (such that $[0 < \theta \leq \pi]$) is equivalent to the knowledge of the Wigner function itself. This Wigner function can be obtained from the set of distributions $w_{\hat{\rho}}(x_\theta, \theta)$ via the inverse Radon transformation:

$$\begin{aligned} W_{\hat{\rho}}(q,p) &= \frac{1}{(2\pi\hbar)^{3/2}} \int_{-\infty}^{\infty} dx_\theta \int_{-\infty}^{\infty} d\xi |\xi| \\ &\times \int_0^\pi d\theta w_{\hat{\rho}}(x_\theta, \theta) \exp \left[\frac{i}{\hbar} \xi (x_\theta - q \cos \theta - p \sin \theta) \right]. \end{aligned} \tag{24}$$

We stress that the transformation (24) is a ‘deterministic’ inverse transformation with the help of which the complete knowledge about the state encoded in the marginal distributions $w_{\hat{\rho}}(x_{\theta}, \theta)$ is rewritten in the form of a Wigner function.

This reconstruction scheme has been used by Raymer and his co-workers [16, 17]. In their experiments the Wigner functions of a coherent state and a squeezed vacuum state have been reconstructed from tomographic data.

Quantum-state tomography can be applied not only to optical fields but also for reconstruction of other physical systems. In particular, Janicke and Wilkens [18] have suggested that Wigner functions of atomic waves can be tomographically reconstructed. Mlynek and co-workers [19] have performed experiments in which Wigner functions of matter wave packets have been reconstructed. Yet another example of the tomographic reconstruction is a reconstruction of Wigner functions of vibrational states of trapped atomic ions theoretically described by a number of groups [20] and experimentally measured by Leibfried and co-workers [21]. Vibrational motional states of molecules have also been reconstructed by this kind of quantum tomography by Dunn *et al.* [22].

The problem with the inverse Radon transformation is that it does not take into account the possibility of finite number of measured distributions. As we will show later, in the case of incomplete tomographic data the transformation (24) can lead to unphysical reconstructions (e.g. non-positive density operators). In what follows we briefly review a quantum tomography scheme which is based on sampling via the pattern functions, which is equivalent to the inverse Radon transformation.

2.1.1. Quantum tomography via pattern functions

In a sequence of papers D’Ariano *et al.* [14], Leonhardt *et al.* [23] and Richter [24] have shown that Wigner functions can be very efficiently reconstructed from tomographic data with the help of the so-called pattern functions. This reconstruction procedure is more efficient than the usual Radon transformation [25]. To be specific, D’Ariano *et al.* [14] have shown that the density matrix ρ_{mn} in the Fock basis can be reconstructed directly from the tomographic data, i.e. from the quadrature-amplitude ‘histograms’ (probabilities), $w(x_{\theta}, \theta)$ via the so-called *direct sampling method* when

$$\rho_{mn} = \int_0^{\pi} \int_{-\infty}^{\infty} w(x_{\theta}, \theta) F_{mn}(x_{\theta}, \theta) dx_{\theta} d\theta, \quad (25)$$

where $F_{mn}(x_{\theta}, \theta)$ is a set of specific *sampling* functions (see below). Once the density matrix elements are reconstructed with the help of equation (25) then the Wigner function of the corresponding state can be directly obtained using the relation

$$W_{\hat{\rho}}(q, p) = \sum_{m,n} \rho_{mn} W_{|m\rangle\langle n|}(q, p), \quad (26)$$

where $W_{|m\rangle\langle n|}(q, p)$ is the Wigner function of the operator $|m\rangle\langle n|$.

A serious problem with the direct sampling method as proposed by D’Ariano *et al.* [14] is that the sampling functions $F_{mn}(x_{\theta}, \theta)$ are difficult to compute. Later D’Ariano and co-workers [23, 26] have simplified the expression for the sampling function and have found that it can be expressed as

$$F_{mn}(x_{\theta}, \theta) = f_{mn}(x_{\theta}) \exp[i(m - n)\theta], \quad (27)$$

where the so-called *pattern* function ‘picks up’ the pattern in the quadrature histograms (probability distributions) $w_{mn}(x_\theta, \theta)$ which just matches the corresponding density-matrix element. Recently Leonhardt *et al.* [25] have shown that the pattern functions $f_{mn}(x_\theta)$ can be expressed as derivatives

$$f_{mn}(x) = \frac{\partial}{\partial x} g_{mn}(x), \tag{28}$$

of functions $g_{mn}(x)$ which are given by the Hilbert transformation

$$g_{mn}(x) = \frac{\mathcal{P}}{\pi} \int_{-\infty}^{\infty} \frac{\psi_m(\zeta)\psi_n(\zeta)}{x - \zeta} d\zeta, \tag{29}$$

where \mathcal{P} stands for the principal value of the integral and $\psi_n(x)$ are the real energy eigenfunctions of the harmonic oscillator, i.e. the normalizable solutions of the Schrödinger equation

$$\left(-\frac{\hbar^2}{2} \frac{d^2}{dx^2} + \frac{x^2}{2} \right) \psi_n(x) = \hbar(n + 1/2)\psi_n(x), \tag{30}$$

(we assume $m = \omega = 1$). Further details of possible applications and discussion devoted to numerical procedures of the reconstruction of density operators via the direct sampling method can be found in [25].

3. MaxEnt principle and quantum tomography

3.1. MaxEnt principle and reconstruction of density operators

Let us assume a set of observables \hat{G}_ν ($\nu = 1, \dots, n$) associated with the quantum system under consideration. This system is prepared in an unknown state $\hat{\rho}$. Let us assume that from a measurement performed over the system mean values G_ν of the observables \hat{G}_ν are found. The task is to determine (estimate) the unknown state of the quantum system based on the results of the measurement. Providing the set of the observables \hat{G}_ν is not equal to the quorum, then the measured mean values do not determine the state uniquely. Specifically, there is a large number of density operators which fulfill the conditions

$$\begin{aligned} \text{Tr } \hat{\rho}_{\{\hat{G}\}} &= 1, \\ \text{Tr } (\hat{\rho}_{\{\hat{G}\}} \hat{G}_\nu) &= G_\nu, \quad \nu = 1, 2, \dots, n. \end{aligned} \tag{31}$$

To estimate the unknown density operator in the most reliable way we utilize the Jaynes principle of maximum entropy (*MaxEnt* principle) [4–7], according to which, among those operators which fulfill constraints (31), the most reliable estimation $\hat{\rho}_{\text{ME}}$ is the one with the maximal value of the von Neumann entropy $S(\hat{\rho}) = -\text{Tr}(\hat{\rho} \ln \hat{\rho})$:

$$S(\hat{\rho}_{\text{ME}}) = \max[S(\hat{\rho}_{\{\hat{G}\}}); \forall \hat{\rho}_{\{\hat{G}\}}]. \tag{32}$$

The operator which fulfills constraints (31) and simultaneously maximizes the von Neumann entropy can be expressed in the generalized canonical form [4, 5, 7, 27]

$$\hat{\rho}_{\text{ME}} = \frac{1}{Z_{\{\hat{G}\}}} \exp \left(- \sum_{\nu} \lambda_{\nu} \hat{G}_{\nu} \right); \tag{33}$$

where

$$Z_{\{\hat{G}\}}(\lambda_1, \dots, \lambda_n) = \text{Tr} \left[\exp \left(- \sum_{\nu} \lambda_{\nu} \hat{G}_{\nu} \right) \right], \quad (34)$$

is the generalized partition function and λ_n are the Lagrange multipliers. The mean values G_{ν} which determine the density operator can be obtained as the derivatives of the partition function

$$G_{\nu} = \text{Tr} (\hat{\rho}_{\text{ME}} \hat{G}_{\nu}) = - \frac{\partial}{\partial \lambda_{\nu}} \ln Z_{\{\hat{G}\}}(\lambda_1, \dots, \lambda_n). \quad (35)$$

If we solve the last equation with respect to the Lagrange multipliers we can express them in terms of the measured mean values

$$\lambda_{\nu} = \lambda_{\nu}(G_1, \dots, G_n). \quad (36)$$

When we substitute the Lagrange multipliers (36) into the expression for the generalized canonical density operator (33) we obtain the explicit expression for the estimated density operator.

3.2. Quantum tomography via the MaxEnt principle

The probability density distribution $w_{\hat{\rho}}(x_{\theta})$ (see equation (9)) for rotated quadratures \hat{x}_{θ} can be represented as a result of the measurement of the continuous set of projectors $|x_{\theta}\rangle\langle x_{\theta}|$. Based on the measurement of the distributions $w_{\hat{\rho}}(x_{\theta})$ for all values of $\theta \in [0, \pi]$ we can reconstruct the density operator according to the formula

$$\hat{\rho}_{\text{ME}} = \frac{1}{Z_0} \exp \left[- \int_0^{\pi} d\theta \int_{-\infty}^{\infty} dx_{\theta} |x_{\theta}\rangle\langle x_{\theta}| \lambda(x_{\theta}) \right], \quad (37)$$

where the Lagrange multipliers $\lambda(x_{\theta})$ are given by an infinite set of equations

$$w_{\hat{\rho}}(x_{\theta}) = (2\pi\hbar)^{1/2} \langle x_{\theta} | \hat{\rho}_{\text{ME}} | x_{\theta} \rangle; \quad \forall x_{\theta} \in (-\infty, \infty). \quad (38)$$

If the distributions $w_{\hat{\rho}}(x_{\theta})$ are measured for all values of x_{θ} and all angles θ then the density operator $\hat{\rho}_{\text{ME}}$ is reconstructed precisely and is equal to a density operator obtained with the help of the inverse Radon transformation (or with the help of the pattern functions).

In a practical experimental situation (see the experiments by Raymer *et al.* [16] and by Mlynek and co-workers [19]) it is impossible to measure the distributions $w_{\hat{\rho}}(x_{\theta})$ for all values of x_{θ} and all angles θ . What is measured are distributions (histograms) for a finite number N_{θ} of quadrature angles θ and the finite number N_x of bins for quadrature operators. This means that practical experiments are associated with an observation level specified by a finite number of observables

$$\hat{Q}_{nm} = |x_{\theta_m}^{(n)}\rangle\langle x_{\theta_m}^{(n)}| \quad (39)$$

with the number of quadrature angles equal to N_{θ} and the number of bins for each quadrature equal to N_x . These observables in the Fock basis can be represented as

$$(\hat{Q}_{nm})_{k_1, k_2} = \psi_{k_1}^*(x_n) \psi_{k_2}(x_n) \exp[i\theta_m(k_1 - k_2)], \quad (40)$$

where θ_m is the quadrature phase, x_n is eigenvalue of the quadrature operator and $\psi_k(x)$ is the wavefunction of the k th energy eigenstate (Fock state) of the harmonic

oscillator. We can therefore assume that from the measurement of the observables \hat{Q}_{nm} the mean values \bar{Q}_{nm} are determined (these mean values correspond to ‘discretized’ quadrature distributions). In addition it is usually the case that the mean photon number of the state is known (measured) as well.

The operators \hat{Q}_{nm} together with \hat{n} form a specific observation level corresponding to the incomplete tomographic measurement. In this case we can express the generalized canonical density operator in the form

$$\hat{\rho}_{\text{ME}} = \frac{1}{Z} \exp \left(-\lambda_0 \hat{n} - \sum_{n=1}^{N_x} \sum_{m=1}^{N_\theta} \lambda_{n,m} |x_{\theta_m}^{(n)}\rangle \langle x_{\theta_m}^{(n)}| \right). \quad (41)$$

The knowledge of the mean photon number is essential for the *MaxEnt* reconstruction because it formally regularizes the *MaxEnt* reconstruction scheme (the general partition function is finite in this case).

4. Numerical implementation

Let us summarize what is supposed to be known as a result of the measurement—these are the measured mean values \bar{Q}_{nm} and \bar{n} of the observables \hat{Q}_{nm} and \hat{n} , respectively. Further, the experimental setup gives us the numbers N_θ and N_x as well as the size Δx of the quadrature bins. These last two numbers specify the range of measured quadratures $-N_x \Delta x / 2 \leq x \leq N_x \Delta x / 2$.

In addition to these ‘experimental’ parameters we have to specify also the dimensionality N_{max} of the Hilbert space in which we reconstruct the density operator. In the case of the *MaxEnt* reconstruction N_{max} has to be chosen so that the ‘truncation’ of the Hilbert space does not affect the reconstruction of the state of the original light field (i.e. $N_{\text{max}} \gg \bar{n}$ so that the reconstructed state ‘fits’ into the truncated Hilbert space).

To perform the reconstruction we have to determine the Lagrange multipliers $\lambda_{n,m}$ in the expression for the generalized canonical density operator (41). These multipliers are given by constraints (31) and numerically can be determined via the minimization of a deviation function ΔQ with respect to the measured mean photon number \bar{n} and the set of histograms $\hat{Q}_{nm} = \text{Tr} \{ \hat{\rho} \hat{Q}_{nm} \}$:

$$\Delta Q = (\bar{n} - \text{Tr} \{ \hat{\rho}_{\text{ME}} \hat{n} \})^2 + \sum_{n,m=1}^{N_\theta, N_x} (\bar{Q}_{nm} - \text{Tr} \{ \hat{\rho}_{\text{ME}} \hat{Q}_{nm} \})^2. \quad (42)$$

The trace is performed within the truncated Hilbert space specified by the parameter N_{max} . When $\Delta Q = 0$ the Lagrange multipliers are determined precisely and the reconstructed density operator $\hat{\rho}_{\text{ME}}$ ideally satisfies the mean values of the measured observables. In the case of incompatible observations [28] the minimum of ΔQ (least squares) yield a good physical estimate. Alternatively, the maximum likelihood estimation can be efficiently used [28].

In order to find the minimal value of the function ΔQ and to determine the Lagrange multipliers we utilize the Levenberg–Marquardt algorithm with a finite difference Jacobian (see a standard routine from the IMSL library, Visual Numerics, Inc., <http://www.vni.com>).

Once the Lagrange multipliers are specified then using the expression for the generalized canonical density operator (41) we can plot the corresponding Wigner

function. The fidelity of the reconstruction is given by three parameters. First, it is the minimal value of the function ΔQ which determines the deviation between the measured mean values of the observables and the corresponding mean values evaluated from the reconstructed density operator. Secondly, if it is *a priori* known that the measured system is prepared in a pure state then the von Neumann entropy S of the density operator $\hat{\rho}_{\text{ME}}$ is a measure of the fidelity of the reconstruction. Specifically, if the entropy is equal to zero then the pure state is perfectly reconstructed. Thirdly, if we want to test the reconstruction scheme we can compare the reconstructed density operator with the known original $\hat{\rho}$. In this case we can use the measure

$$\Delta\rho = \sum_{m,n}^{N_x N_\theta} |(\hat{\rho})_{mn} - (\hat{\rho}_{\text{ME}})_{mn}|^2. \quad (43)$$

Let us test the *MaxEnt* reconstruction scheme and assume the mean values of the observables \hat{Q}_{mn} to be given by the even coherent state (11) with the real amplitude $\alpha = 2$ (we plot the Wigner function of this state in figure 1 (a)). Let us further assume just two quadrature angles $N_\theta = 2$ corresponding to the measurement of the position and the momentum of the harmonic oscillator. The total number of bins for each quadrature is taken to be $N_x = 40$ with the size of the bin equal to $\Delta x = 0.2$ (we assume $\hbar = 1$) which corresponds to the measurement of the quadrature distributions on the interval $\langle -4, 4 \rangle$. For the given mean photon number ($\bar{n} \simeq 4$) it is enough to consider the Hilbert space of the dimension $N_{\text{max}} = 20$. The even coherent state with $\alpha = 2$ can be very well approximated as a superposition of even number states up to $n = 8$ (the higher number states are occupied with 1% probability), so $N_{\text{max}} = 20$ is a very good truncation.

With these values of the parameters we have performed the reconstruction of the state via the *MaxEnt* principle. Using the minimization procedure we have achieved the deviation, with respect to the 'experimental' data, $\Delta Q = 5.4 \times 10^{-12}$. The difference between the reconstructed density operator and the original measured in terms of (43) in this particular case is $\Delta\rho = 1.0 \times 10^{-10}$. We see that the reconstruction is indeed very precise even for a very small number of experimental data. The high quality of the reconstruction is indicated by the corresponding value of the von Neumann entropy $S \approx 10^{-6}$. We plot the reconstructed Wigner function in figure 1 (b). From this figure we see that the reconstruction and the original are essentially identical. We also note that the quality of the reconstruction practically does not depend on the choice of N_{max} when this is larger than some minimal value related to \bar{n} (in our case for $N_{\text{max}} > 12$ the reconstruction is almost perfect but even for $N_{\text{max}} = 8$ the fidelity is very high).

In order to illustrate the *MaxEnt* reconstruction scheme for statistical mixtures we will consider briefly a statistical mixture described by the density operator

$$\hat{\rho} = \frac{1}{2}|\alpha\rangle\langle\alpha| + \frac{1}{2}|-\alpha\rangle\langle-\alpha| \quad (44)$$

with a real amplitude $\alpha = 2$. The Wigner function of this state is plotted in figure 2 (a). In figure 2 (b) we plot the reconstructed Wigner function under the same conditions as figure 1 (b), i.e. $N_\theta = 2$, $N_x = 40$, $\Delta x = 0.2$ and $N_{\text{max}} = 20$. The two measured quadratures are the position and the momentum. We see from the

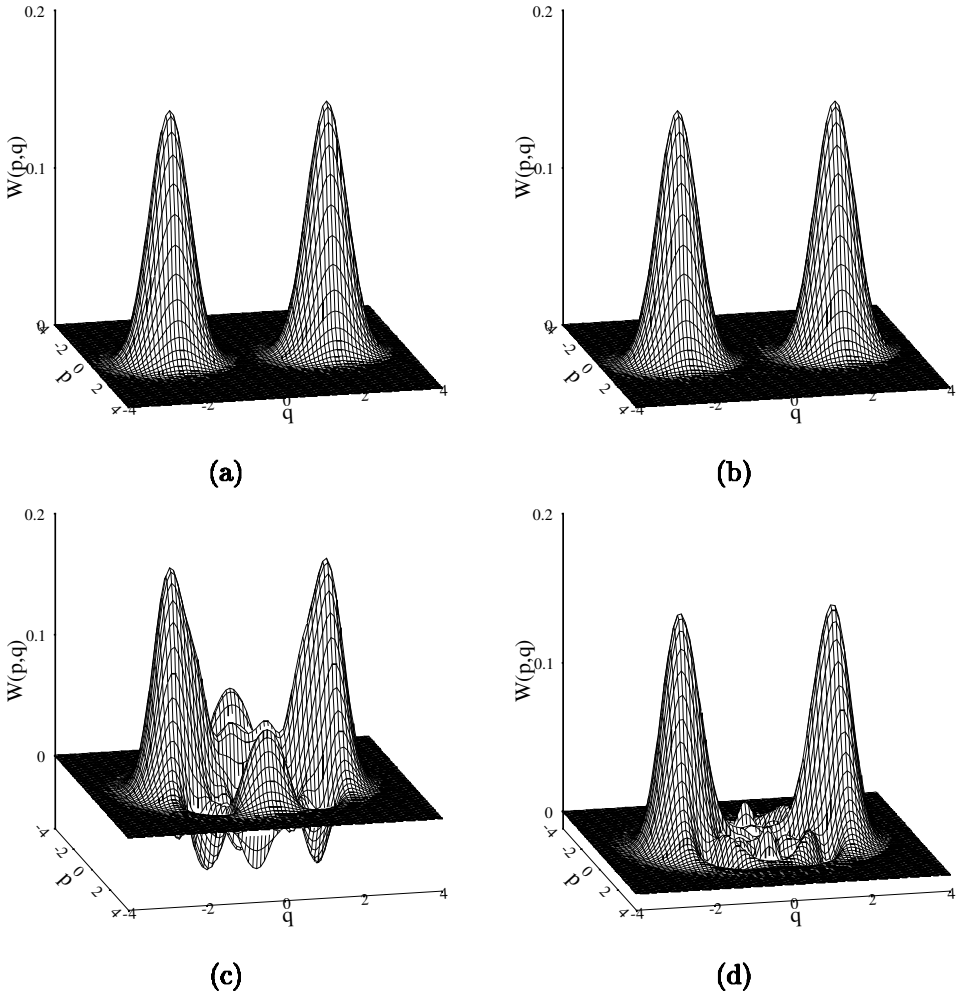


Figure 2. (a) The Wigner function of the mixture of two coherent states with $\alpha = \pm 2$. (b) The reconstruction of the Wigner function via the *MaxEnt* principle based on the measurement of marginal distributions for the position and the momentum ($N_\theta = 2$). The measured marginal distributions are divided into $N_x = 40$ bins of width $\Delta x = 0.2$ covering the interval $(-4, 4)$. The fidelity of the reconstruction is $\Delta Q = 1.4 \times 10^{-8}$ and $\Delta \rho = 1.1 \times 10^{-8}$, with entropy $S = 0.694$. (c) The tomography via pattern functions with $N_\theta = 4$ and $N_{\max} = 8$ for which the minimum deviation $\Delta Q = 0.71$ is obtained. The fidelity of the reconstruction is $\Delta \rho = 0.17$. The reconstructed density operator is unphysical. (d) For the larger number of quadratures $N_\theta = 8$ with $N_{\max} = 8$ we obtain $\Delta Q = 0.13$ and $\Delta \rho = 0.023$. The reconstructed Wigner function still exhibits some fictitious interference structure.

figure that the reconstruction is almost perfect. For this reconstruction we have $\Delta Q = 1.4 \times 10^{-8}$ and $\Delta \rho = 1.1 \times 10^{-8}$. The corresponding entropy $S = 0.694$ is close to $\ln 2$.

Here we note that the size of the bin Δx does not play a significant role in the reconstruction via the *MaxEnt* principle. We will discuss this issue in more detail below, but now we concentrate our attention on role of the number N_θ of the quadrature angles.

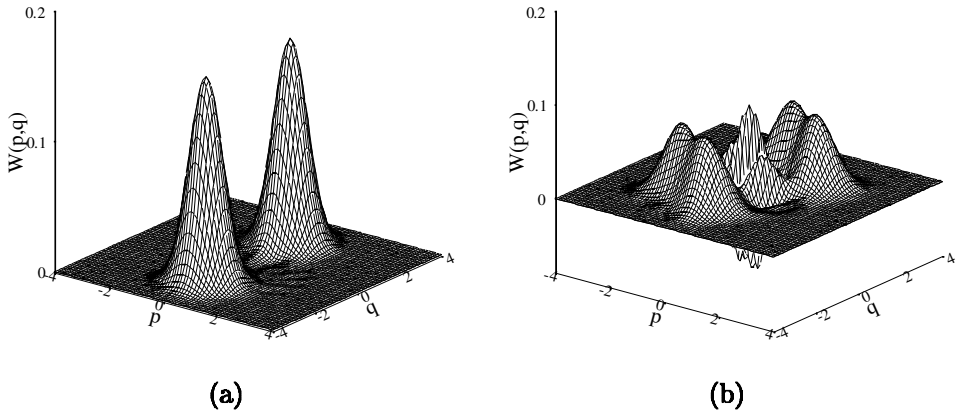


Figure 3. The Wigner function of the even coherent state $\alpha = 2$ reconstructed via the *MaxEnt* principle from two particular marginal distributions ($N_\theta = 2$). In (a) we consider two rotated quadratures for $\theta = 0$ and $\theta = \pi/8$. The reconstruction leads to a statistical mixture of two coherent states. The fidelity of the reconstruction is $\Delta Q \approx \times 10^{-6}$, $\Delta\rho = 0.49$, and the entropy is $S = 0.7$. (b) The choice of ‘measurement angles’ $\theta = \pi/8, \pi/2 + \pi/8$ leads to a mixture with $\Delta Q \approx \times 10^{-7}$, $\Delta\rho = 0.60$ and the entropy is $S = 1.31$. Other settings (the number of bins and their width) are the same as in figure 1.

4.1. Minimal number of measured quadratures

The two quadratures $\hat{q} = \hat{x}_{\theta=0}$ and $\hat{p} = \hat{x}_{\theta=\pi/2}$ are sufficient for a reconstruction of the even coherent state when α is real (this corresponds a specific *a priori* information about the state). If we consider the most general case, when α is complex, then the reconstruction based on the measurement of just two quadratures is not very good (in what follows, instead of choosing the complex α , we will use the corresponding rotated quadratures).

First, let us consider a reconstruction of the even coherent state with the real amplitude α based on the measurement of two rotated quadratures which are not mutually orthogonal. In particular, let us assume $\hat{x}_{\theta=0}$ and $\hat{x}_{\theta=\pi/8}$. The other settings are the same as in figure 1 (b). We plot the reconstructed Wigner function in figure 3 (a). It is very similar to the Wigner function of the statistical mixture (which is also indicated by the value of the corresponding von Neumann entropy close to $\ln 2$). The reason is that the type of measurement considered in the example does not provide us with enough information about the interference pattern in the phase space (the two measured quadratures are ‘too’ close).

Our next example is the case when the two measured quadratures are mutually orthogonal, but are rotated with respect to the position and the momentum. Specifically, $\hat{x}_{\theta=\pi/8}$ and $\hat{x}_{\theta=\pi/2+\pi/8}$ and the other settings are the same as in figure 1 (b). We plot the reconstructed Wigner function in figure 3 (b). In this Wigner function we see some interference pattern but the information from the measurement does not allow us to perform a reliable reconstruction ($\Delta Q \approx 10^{-7}$, $\Delta\rho = 0.60$, and $S = 1.31$). We can observe some ‘fictitious’ peaks in the reconstructed Wigner function.

To improve the fidelity of the reconstruction we have to consider a larger number of the rotated quadratures. In fact, it is our empirical experience that three rotated quadratures ($N_\theta = 3$) are always sufficient to perform a very reliable

MaxEnt reconstruction of an arbitrary unknown state. We have not found yet a rigorous proof for this empirical observation.

4.2. Comparison with the reconstruction via direct sampling

It has been shown by Leonhardt and co-workers [25, 28] that for a reliable reconstruction via direct sampling with the help of the pattern functions two conditions have to be satisfied:

$$\begin{aligned} N_\theta &= N_{\max}, \\ \Delta x &< \pi/2(2N_{\max} + 1)^{1/2}. \end{aligned} \tag{45}$$

This means that the truncation of the Hilbert space in which the reconstructed density operator is defined specifies how many quadrature angles have to be considered as well as putting some restriction on the size of the bin.

4.2.1. The role of N_θ

We start with the analysis of the first condition. In our case of the even coherent state with $\alpha = 2$ we have to consider at least $N_{\max} = 8$. Consequently, following Leonhardt and co-workers we would have to consider a measurement of $N_\theta = 8$ quadratures. In this case the precision of reconstruction via the direct sampling using pattern functions is $\Delta Q = 0.13$ and $\Delta\rho = 0.03$ which is reasonable, but much smaller than in the case of the *MaxEnt* reconstruction. It is important to remember that any deviation of N_θ from N_{\max} causes a dramatic deterioration of the reconstruction scheme (for more details see [25, 28]). In particular, for $N_{\max} > N_\theta$ higher ‘ghost’ Fock states appear in the reconstructed density matrix. This effect of aliasing (see [28]) is caused by the fact that in the sampling method the matrix elements ρ_{mn} with $(m - n) \bmod N_\theta$ cannot be distinguished.

To see the effect of an insufficient number of phases for the sampling via pattern functions we plot in figure 1 the results for $N_\theta = 2$ (see figure 1 (c)) and $N_\theta = 4$ (see figure 1 (d)) marginal distributions. In both cases we chose N_{\max} such that the parameter ΔQ (deviation from the measured data) is minimized. In particular, for $N_\theta = 2$ using the numerical search we have found that ΔQ is minimized for $N_{\max} = 4$ when $\Delta Q = 9.17$ and $\Delta\rho = 3.7$. However, the reconstructed density operator is unphysical—we obtain *negative* probabilities of odd Fock states: $P_1 = -0.35$, $P_3 = -0.54$. The corresponding Wigner function is plotted in figure 1 (c). Analogously, for $N_\theta = 4$ we have found the optimal truncation to be $N_{\max} = 6$. In this case $\Delta Q = 1.33$ and $\Delta\rho = 0.51$. The fidelity of the reconstruction is now better, but it still gives us an unphysical result with $P_1 = -0.1$ (the corresponding Wigner function is plotted in figure 1 (d)). We have checked that higher values of N_{\max} significantly deteriorate the quality of reconstructions. Comparing the sampling method with the result of the *MaxEnt* approach we see the great advantage of the later for a small number of quadrature phases.

Analogous results are obtained also for statistical mixtures (see figure 2). Specific values for the fidelities of the reconstruction are given in the figure caption.

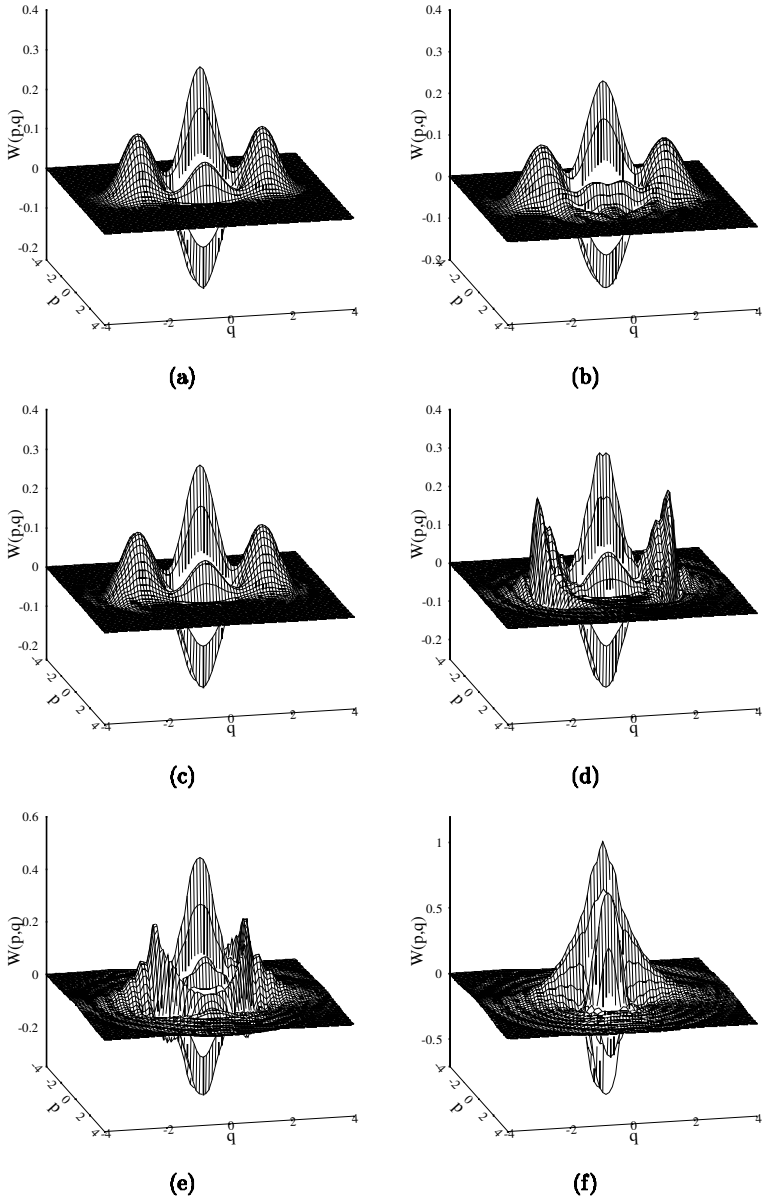


Figure 4. The reconstruction of the Wigner function of the even coherent state with $\alpha=2$. (a) The reconstruction via the *MaxEnt* principle with two marginal distributions ($N_\theta=2$) for the position and the momentum. The ‘measured’ marginal distributions are divided into $N_x=20$ bins of width $\Delta x=0.2$ covering the interval $\langle -2,2 \rangle$. The fidelity of the reconstruction is $\Delta Q=2 \times 10^{-15}$ and $\Delta \rho=2 \times 10^{-10}$ which is comparable with figure 1 (b) (where $N_x=40$ corresponding to $x \in \langle -4,4 \rangle$). (b) This is the same example as (a) except $N_x=10$, i.e. $x \in \langle -1,1 \rangle$. The quality of the reconstruction decreases to $\Delta Q=3 \times 10^{-15}$ and $\Delta \rho=0.029$. (c)–(f) Reconstruction via pattern functions with $N_\theta=20$ and $N_{\max}=20$. The marginals are taken within the intervals (c) $\langle -4,4 \rangle$ [$\Delta Q=0.05$, $\Delta \rho=0.002$]; (d) $\langle -3,3 \rangle$ [$\Delta Q=0.88$, $\Delta \rho=0.154$]; (e) $\langle -2,2 \rangle$ [$\Delta Q=8.6$, $\Delta \rho=1.01$]; (f) $\langle -1,1 \rangle$ [$\Delta Q=47.7$, $\Delta \rho=5.82$]. We see that the shorter the interval on which the quadrature distribution is measured, the less reliable the reconstruction is.

4.2.2. The role of N_x

In addition to the required resolution of bins, i.e. $\Delta x < \pi/2(2N_{\max} + 1)^{1/2}$, the sampling via pattern functions is also very sensitive with respect to the size of the interval on which the marginals are measured. To apply the sampling via pattern functions marginal distributions have been measured on the whole interval where they take non-zero values. The importance of the distribution 'tails' of the marginals can be illustrated on the example of the even coherent state. Let us consider the size of the bin (i.e. the resolution) to be $\Delta x = 0.2$ and let us change the values of N_x .

In figure 4 we plot the reconstructed Wigner functions which are obtained from the incomplete marginal distributions via the *MaxEnt* (figures 4 (a) and (b)) and via the sampling (figures 4 (c)–(f)) reconstruction schemes.

In figure 4 (a) we plot the reconstruction via the *MaxEnt* principle with two marginal distributions ($N_\theta = 2$). The 'measured' marginal distributions are divided into $N_x = 20$ bins of width $\Delta x = 0.2$ covering the interval $\langle -2, 2 \rangle$. The quality of the reconstruction is $\Delta Q = 2 \times 10^{-15}$, $\Delta \rho = 2 \times 10^{-10}$, and $S \approx 10^{-8}$ which is comparable with figure 1 (b) when $N_x = 40$ and $x \in \langle -4, 4 \rangle$. We see that even though the interval on which the marginal distributions are measured is shorter by a factor of two the fidelity of reconstruction is not affected. In figure 4 (b) we plot the reconstructed Wigner function under the same conditions except $N_x = 10$, i.e. $x \in \langle -1, 1 \rangle$. The quality of the reconstruction decreases to $\Delta Q = 3 \times 10^{-15}$, $\Delta \rho = 0.029$ and $S = 0.20$, but still is rather reliable.

In figures 4 (c)–(f) we present results of the reconstruction via the direct sampling. We assume $N_\theta = 20$ and $N_{\max} = 20$. That is, we consider significantly more data than in the previous two cases. Nevertheless, results of the reconstruction are much worse. Specifically, let us assume the marginal distributions to be taken within the intervals (c) $\langle -4, 4 \rangle$ which results in the reconstruction with the fidelity $\Delta Q = 0.05$ and $\Delta \rho = 0.002$. Analogously, (d) $\langle -3, 3 \rangle$ with $\Delta Q = 0.88$, $\Delta \rho = 0.154$; (e) $\langle -2, 2 \rangle$ with $\Delta Q = 8.6$, $\Delta \rho = 1.01$; (f) $\langle -1, 1 \rangle$ with $\Delta Q = 47.7$, $\Delta \rho = 5.82$. We conclude that the shorter the interval on which the quadrature distribution is measured, the less reliable the reconstruction is. From figure 4 it is seen that the sampling via pattern functions can reconstruct only a structure within a measured region of the phase space.

From above we can conclude that for a reliable use of the reconstruction via the direct sampling we have to measure a sufficient number of quadrature distributions ($N_\theta = N_{\max}$) on the whole interval of x . Conversely, with the *MaxEnt* approach we need just a small number of quadrature distributions and the interval on which the distributions are measured can be rather small. We have also analysed the situation when the distributions are measured on the interval which is not symmetric with respect to the origin of the phase space. In this case the *MaxEnt* scheme works very reliably while the direct sampling fails completely.

5. Conclusions

We have shown that the reconstruction of Wigner functions from incomplete tomographic data can be very reliably performed with the help of the Jaynes principle of Maximal Entropy. We have presented a generalized canonical density operator which is suitable for the incomplete tomographic data. We have implemented a numerical procedure with the help of which the *MaxEnt* reconstruc-

tion can be performed. We have compared the *MaxEnt* scheme with the sampling via pattern functions. The comparison is very clear—the *MaxEnt* approach is much more efficient. It requires less data, it gives the reconstruction with much higher fidelity and is more stable with respect to the choice of parameters such as the size of the quadrature bin, or the interval on which the quadrature distributions are measured. Our empirical experience shows that three rotated quadratures are always sufficient to perform a very reliable *MaxEnt* reconstruction of an arbitrary unknown state. The method presented in this paper can be applied to various quantum systems. We plan to adopt it for the reconstruction of Wigner functions of vibrational states of neutral atoms based on the experimental data obtained in the group of Salomon [29].

Acknowledgments

We thank Harald Wiedemann and Peter Knight for helpful discussions. This work was supported in part by the IST project QUBITS under the contract IST-1999-13021.

References

- [1] BALLENTINE, L. E., 1990, *Quantum Mechanics* (Englewood Cliffs, NJ: Prentice Hall).
- [2] BAND, W., and PARK, J. L., 1979, *Am. J. Phys.*, **47**, 188; 1970, *Found. Phys.*, **1**, 133; 1971, *Found. Phys.*, **1**, 339; PARK, J. L., and BAND, W., 1971, *Found. Phys.*, **1**, 211.
- [3] NEWTON, R. G., and YOUNG, B. L., 1968, *Ann. Phys.* (New York), **49**, 393.
- [4] JAYNES, E. T., 1957, *Phys. Rev.*, **108**, 171; 1957, *ibid.*, **108**, 620; 1963, *Am. J. Phys.*, **31**, 66.
- [5] FICK, E., and SAUERMAN, G., 1990, *The Quantum Statistics of Dynamic Processes* (Berlin: Springer Verlag).
- [6] KAPUR, J. N., and KESAVAN, H. K., 1992, *Entropic Optimization Principles with Applications* (New York: Academic Press).
- [7] KATZ, A., 1967, *Principles of Statistical Mechanics* (San Francisco: W. H. Freeman and Company); HOBSON, A., 1971, *Concepts in Statistical Mechanics* (New York: Gordon Breach Science Publishers).
- [8] WIGNER, E. P., 1932, *Phys. Rev.*, **40**, 749; see also HILLERY, M., O'CONNELL, R. F., SCULLY, M. O., and WIGNER, E. P., 1984, *Phys. Rep.*, **106**, 121.
- [9] BUZEK, V., VIDIELLA-BARRANCO, A., and KNIGHT, P. L., 1992, *Phys. Rev. A*, **45**, 6570; BUZEK, V., and KNIGHT, P. L., 1995, *Progress in Optics*, Vol. 34, edited by E. Wolf (Amsterdam: North Holland), p. 1.
- [10] EKERT, A. K., and KNIGHT, P. L., 1991, *Phys. Rev. A*, **43**, 3934.
- [11] VOGEL, K., and RISKEN, H., 1989, *Phys. Rev. A*, **40**, 2847; see also BERTRAND, J., and BERTRAND, P., 1987, *Found. Phys.*, **17**, 397; FREYBERGER, M., VOGEL, K., and SCHLEICH, W. P., 1993, *Phys. Lett. A*, **176**, 41; AGARWAL, G. S., and CHATURVEDI, S., 1994, *Phys. Rev. A*, **49**, R665; VOGEL, W., and WELSCH, D.-G., 1995, *Acta Phys. Slov.*, **45**, 313; LEONHARDT, U., and PAUL, H., 1994, *Phys. Lett. A*, **193**, 117; LEONHARDT, U., and PAUL, H., 1994, *J. mod. Optics*, **41**, 1427; LEONHARDT, U., 1993, *Phys. Rev. A*, **48**, 3265; LEONHARDT, U., and PAUL, H., 1993, *Phys. Rev. A*, **48**, 4598; PAUL, H., LEONHARDT, U., and D'ARIANO, G. M., 1995, *Acta Phys. Slov.*, **45**, 261.
- [12] LEONHARDT, U., 1997, *Measuring the Quantum State of Light* (Cambridge: Cambridge University Press).
- [13] WELSCH, D.-G., VOGEL, W., and OPATRYNY, T., 1999, *Progress in Optics XXXIX*, edited by E. Wolf (Amsterdam: North Holland), p. 63.
- [14] D'ARIANO, G. M., MACHIAVELO, C., and PARIS, M. G. A., 1994, *Phys. Rev. A*, **50**, 4298.
- [15] KÜHN, H., WELSCH, D.-G., and VOGEL, W., 1994, *J. mod. Optics*, **41**, 1607.

- [16] SMITHEY, D. T., BECK, M., RAYMER, M. G., and FARIDANI, A., 1993, *Phys. Rev. Lett.*, **70**, 1244; SMITHEY, D. T., BECK, M., COOPER, J., and RAYMER, M. G., 1993, *Phys. scripta T*, **48**, 35; BECK, M., RAYMER, M. G., WALMSLEY, I. A., and WONG, V., 1993, *Optics Lett.*, **18**, 2041; BECK, M., SMITHEY, D. T., and RAYMER, M. G., 1993, *Phys. Rev. A*, **48**, R890; RAYMER, M. G., BECK, M., and MCALISTER, D. F., 1994, *Phys. Rev. Lett.*, **72**, 1137; RAYMER, M. G., SMITHEY, D. T., BECK, M., and COOPER, J., 1994, *Acta Phys. Pol.*, **86**, 71.
- [17] MUNROE, M., BOGGAVARAPU, D., ANDERSON, M. E., and RAYMER, M. G., 1995, *Phys. Rev. A*, **52**, R924.
- [18] JANICKE, U., and WILKENS, M., 1995, *J. mod. Optics*, **42**, 2183.
- [19] SCHILLER, S., BREITENBACH, G., PEREIRA, S. F., MULLER, T., and MLYNEK, J., 1996, *Phys. Rev. Lett.*, **77**, 2933; KURTSIEFER, CH., PFAU, T., and MLYNEK, J., 1997, *Nature*, **386**, 150.
- [20] WALLENTOWITZ, S., and VOGEL, W., 1995, *Phys. Rev. Lett.*, **75**, 2932; POYATOS, J. F., WALSER, R., CIRAC, J. I., ZOLLER, P., and BLATT, R., 1996, *Phys. Rev. A*, **53**, R1966; D'HELON, C., and MILBURN, G. J., 1996, *Phys. Rev. A*, **53**, R25.
- [21] LEIBFRIED, D., MEEKHOF, D. M., KING, B. E., MONROE, C., ITANO, W. M., and WINELAND, D. J., 1996, *Phys. Rev. Lett.*, **77**, 4281; LEIBFRIED, D., MEEKHOF, D. M., MONROE, C., KING, B. E., ITANO, W. M., and WINELAND, D. J., 1997, *J. mod. Optics*, **44**, 2485; WINELAND, D., MONROE, C., MEEKHOF, D. M., KING, B. E., LIEBFRIED, D., ITANO, W. M., BERGQUIST, J. C., BERKELAND, D., BOLLINGER, J. J., and MILLER, J., 1998, *Proc. Roy. Soc. A*, **454**, 411.
- [22] DUNN, T. J., WALMSLEY, I. A., and MUKAMEL, S., 1995, *Phys. Rev. Lett.*, **74**, 884.
- [23] LEONHARDT, U., PAUL, H., and D'ARIANO, G. M., 1995, *Phys. Rev. A*, **52**, 4899.
- [24] RICHTER, TH., 1996, *Phys. Lett. A*, **211**, 327; RICHTER, TH., 1996, *Phys. Rev. A*, **53**, 1197.
- [25] LEONHARDT, U., MUNROE, M., KISS, T., RICHTER, T., and RAYMER, M. G., 1996, *Optics Commun.*, **127**, 144.
- [26] D'ARIANO, G. M., LEONHARDT, U., and PAUL, H., 1995, *Phys. Rev. A*, **52**, R1801.
- [27] BUŽEK, V., ADAM, G., and DROBNÝ, G., 1996, *Ann. Phys. (New York)*, **245**, 37; BUŽEK, V., ADAM, G., and DROBNÝ, G., 1996, *Phys. Rev. A*, **54**, 801; BUZYEK, V., DROBNÝ, G., DERKA, R., ADAM, G., and WIEDEMAN, H., 1999, *Chaos, Solitons Fractals*, **10**, 981.
- [28] HRADIL, Z., SUMMHAMMER, J., and RANCH, H. 2000, *Phys. Lett. A* **261**, 20.
- [29] LEONHARDT, U., and MUNROE, M., 1996, *Phys. Rev. A*, **54**, 3682.
- [30] MORINAGA, M., BOUCHOULE, I., KARAM, J.-C., and SALOMON, C., 1999, *Phys. Rev. Lett.*, **83**, 4037.